JOURNAL OF SOLID STATE CHEMISTRY 73, 480–487 (1988)

Synthesis and Structural Characterization of $CaTiO_3$ Doped with 0.05–7.5 Mole% Gadolinium(III)

ELIZABETH M. LARSON, P. GARY ELLER,* JOHN D. PURSON, AND CHARLES F. PACE

Isotope and Nuclear Chemistry Division, Los Alamos National Laboratory, MS C346, Los Alamos, New Mexico 87545

MICHAEL P. EASTMAN

Department of Chemistry, University of Texas at El Paso, El Paso, Texas 79968

AND R. B. GREEGOR AND F. W. LYTLE

Boeing Corporation, Seattle, Washington 98124

Received April 15, 1987; in revised form September 25, 1987

Titanates containing 0.05–7.5 mole% gadolinium(III) in the $CaTiO_3$ perovskite lattice have been prepared and characterized by X-ray diffraction and absorption, electron paramagnetic resonance, and Raman methods. The structural studies confirm the predicted site substitution of Gd^{3+} ions into the Ca^{2+} sites and suggest charge compensation by a cation deficiency mechanism (Ca^{2+} and/or Ti^{4+} vacancies). Evidence is presented for a significant difference between local Gd^{3+}-substituted sites and the average Ca(Gd) sites, resulting from the difference in charge and size of the two ions. A least-squares refinement of single-crystal X-ray data was carried out on $(Ca_{0.925}Gd_{0.075})TiO_3$, with resulting cell parameters and major structural features within three standard deviations of those previously found for stoichiometric $CaTiO_3$: space group *Pbnm*, $a = 5.381(1)$, $b = 5.449(1)$, $c = 7.647(1)$ Å, $Z = 4$, $R = 4.1\%$ for 236 reflections with $I \geq 2\sigma(I)$. © 1988 Academic Press, Inc.

Introduction

Calcium titanate, $CaTiO_3$, is one constituent of several titanate ceramic composites which have been proposed as hosts for long-term disposal of high-level nuclear wastes (*1, 2*). Originally, transuranic and fission product elements (including lanthanides) were expected to enter these phases by random substitution, with specific site selectivity being determined by ionic size. Charge balance would be achieved through appropriate substitution by coexisting charge-compensating cations. However, recent studies on several calcium titanates and on related phases have shown that this model is no doubt overly simplistic, particularly at the desired high waste loadings (10% or greater) (*3–8*). A variety of structural techniques have been used to show that complicated cation ordering, shear effects, and even twinning on a unit

* To whom correspondence should be addressed.

0022-4596/88 $3.00

Copyright © 1988 by Academic Press, Inc.
All rights of reproduction in any form reserved.

cell basis can occur, in addition to formation of distinct but closely related phases. In an actual nuclear waste matrix, the situation is likely to be even more complex because of radiation effects and the wide range of ions present to compete for lattice sites, provide charge compensation, and generally drastically different phases (*9*).

In this paper we describe the results of structural studies on a simple model system in which varying amounts of Gd^{3+} are doped into the $CaTiO_3$ perovskite lattice. Because of the similarities of the ionic radii of Ca^{2+} and trivalent/tetravalent actinides and lanthanides, for many titanate waste formulations the calcium site in $CaTiO_3$ is expected to be a major host site for fission product and transuranium elements (*1–3, 9–11*). Calcium titanate containing gadolinium, which occupies the middle position of the lanthanide series, thus affords an ideal site substitution model not only for the lanthanide fission products but also for tri- and tetravalent transuranic elements.

Experimental

Synthesis. Reagent-grade CaO from MCB Chemical Co., Ultrex TiO_2 (rutile) from J. T. Baker Chemical Co., and high-purity Gd_2O_3 (C-type) from Lindsay Chemical Co. were used as starting materials. The gadolinium-doped perovskites were prepared by ballmilling the desired stoichiometric ratios of the oxides (Gd for Ca) in a plastic container for about 1 hr, followed by coldpressing at 0.103 GPa (15,000 psi) and firing in air at 1450°C for 2 weeks. When the resulting products were gradually cooled over a period of 2 weeks, highly crystallized pale-brown samples suitable for single-crystal X-ray study were obtained.

X-ray diffraction studies. The perovskite products were the only phases detected by X-ray powder diffraction (Debye–Scherrer technique). After examining many twinned crystals from the product prepared with 7 mole% Gd starting materials, a single crystal was selected whose diffraction pattern could be indexed with the orthorhombic ($GdFeO_3$-type) perovskite cell (*12, 13*). The space group is *Pbnm* with the cell a = 5.381(1), b = 5.449(1), c = 7.647(1) Å, based on the observed systematic absences and the refinement of 24 diffractometer-indexed reflections ($8.5° \leq 2\theta \leq 28°$) (Mo$K\alpha$ radiation, λ = 0.70930 Å). Diffraction data for a hemisphere of reflections (1392 total) were collected at ambient temperature using an Enraf–Nonius Cad4 automated diffractometer ($2\theta_{max} = 60°$). Following Lorentz polarization and absorption corrections, equivalent reflections were averaged to give 236 unique reflections with $I \geq 2\sigma(I)$ (R_f on averaging = 2.7%). Scattering factors including anomalous dispersion terms were taken from Ref. (*14*). The structure was refined using the published positions for $CaTiO_3$ (*13*) as a starting point. The $CaTiO_3$ atoms were refined anisotropically, with corrections for secondary extinction (*15*), to give R = 8.3% and R_w = 12.2% and unreasonably small thermal parameters for calcium. A difference Fourier synthesis showed substantial excess electron density at the calcium site. When the calculation was repeated, refining the coupled occupancy factors of gadolinium and calcium at the calcium site, the refinement converged with Ca and Gd occupancies of 92.5(2) and 7.5(2)%, respectively. The final agreement factors were R = 4.1% and R_w = 5.0%. A difference Fourier synthesis at this point was quite flat, the principal features being several peaks with heights of about 1.2 e/Å (about one-fifth the height of the oxygen atoms in observed Fourier maps for this structure) scattered randomly throughout the structure. Details of the data workup and refinement procedures, including the computer codes used, may be found in Ref. (*15*) and Table I. Table II gives the final unit cell and atomic parameters from the least-squares refinement, compared

TABLE I

DETAILS OF THE SINGLE-CRYSTAL X-RAY DATA COLLECTION AND STRUCTURE SOLUTION FOR $(Ca_{0.925}Gd_{0.075})TiO_3$

Temperature (°K)	298
Crystal size (mm)	0.10 × 0.10 × 0.10
Space group	*Pbnm*
Z	4
Diffraction type	Enraf–Nonius Cad4
Wavelength	0.70930
$2\theta_{max}$ (deg)	60
Number of reflections for refining lattice parameters	24
Scan range (deg)	0.90
Scan rate (deg/min)	Variable, 16.48°/(3 to 10 min)
a (Å)	5.381(1)
b (Å)	5.449(1)
c (Å)	7.647(1)
V (Å^3)	224.22
ρ_{calc} (g/cm^3)	4.097
Unique reflections	262
Contributing reflections	236
Variables	31
Linear absorption coefficient	59.0 cm^{-1}
Range of transmission factors	0.424–0.436
R ($I \geq 2\sigma(I)$)	0.041
R_w ($I \geq 2\sigma(I)$)	0.050
Extinction parameter (as defined in Ref. (*15*))	$2.6 \times e^{-5}$
Weighting scheme:	$w = 2F_o/\sigma(F_o^2)]^2$

with the values for pure $CaTiO_3$ as determined by neutron powder diffraction. Table III contains selected interatomic distances for $(Ca_{0.925}Gd_{0.075})CaTiO_3$. Final anisotropic thermal parameters and observed/calculated structure factors are contained in supplementary Tables I and II.

X-ray absorption measurements. Extended X-ray absorption fine structure (EXAFS) data were collected at room temperature to k values of about 13 in both the absorption and the fluorescence modes on powdered samples contained in plastic envelopes at the Stanford Synchrotron Radiation Laboratory. Perovskite with doping levels of 0.5 and 7.5% were examined. Details of the data workup procedures were as described in earlier publications (*16*). The EXAFS curves were obtained after application of a cubic spline fitting routine to the raw gadolinium L_{III} edges. Gadolinium sesquioxide (C-type) was used as a model compound for phase extraction. Figure 1 exhibits the EXAFS results for the 7.5% Gd-doped perovskite as well as for the Gd_2O_3 standard. EXAFS curves for the 0.5% doped samples had a poorer signal-to-noise ratio, but were otherwise essentially identical, showing that the Gd site environment is the same at these two doping levels.

Raman spectra. Raman data were obtained on powdered samples contained in glass capillaries. Spex Model 1403 spectrometers and Kr and Ar ion lasers (6471, 5145, and 4880 Å lines) were employed. Figure 2 shows the spectra obtained for the perovskites doped at the 0.0, 0.5, and 7.5% doping levels and Table IV summarizes the observed frequencies for undoped $CaTiO_3$. Due to the complexity of the spectra, band assignments were not attempted.

Electron paramagnetic resonance spectra. Electron paramagnetic resonance

TABLE II

FINAL UNIT CELL AND ATOMIC PARAMETERS FOR $(Ca_{0.925}Gd_{0.075}TiO_3)$

	a (Å)	*b* (Å)	*c* (Å)	*V* (Å^3)
$CaTiO_3$[a]	5.3829(3)	5.4458(3)	7.6453(3)	224.12
$(Ca_{0.925}Gd_{0.075})TiO_3$	5.381(1)	5.449(1)	7.647(1)	224.22
	x	*y*	*z*	B_{iso}[b]
Ca(Gd)	0.0066(2)	0.0350(2)	¼	0.97
Ti	½	0	0	0.46
O1	0.5689(9)	−0.0150(8)	¼	0.46
O2	0.2870(6)	0.2870(5)	0.0350(2)	0.76

[a] Reference (*13*).
[b] $B_{iso} = \frac{4}{3}\sum_i\sum_j \beta_{ij}\, a_i a_j$; $\beta_{ij} = 2\pi^2\, u_{ij} a_i^* a_j^*$; u_{ij} = atom displacement (Å^2).

TABLE III

INTERATOMIC DISTANCES AND ANGLES FOR $(Ca_{0.925}Gd_{0.075})TiO_3$

	Ti–O (Å)	Ca(Gd)–O (Å)	O–Ti–O (°)
O1	1.949(1) × 2	2.371(5)	89.2(1)–90.5(1)
O1′		2.485(5)	
O2	1.952(3) × 2	2.614(4) × 2	
O2′	1.959(3) × 2	2.394(4) × 2	
O2″		2.670(4) × 2	

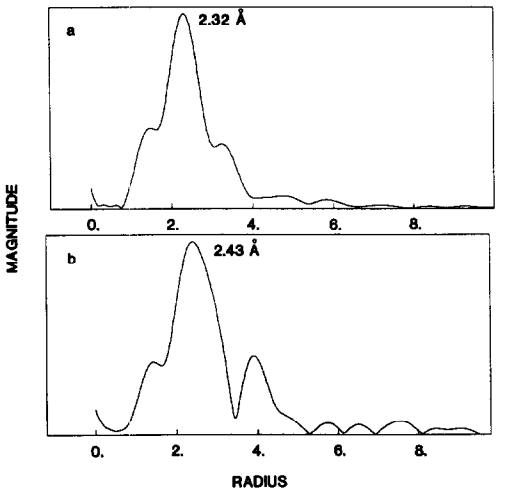

FIG. 1. Phase-corrected radial distribution curves for C-type Gd_2O_3 (a) and $(Ca_{0.925}Gd_{0.075})TiO_3$ (b), derived from Gd L_{III} EXAFS data. Transforms were calculated with k^1 weighting and Gd–O phases were obtained from the first-neighbor distance (2.32 Å as determined by X-ray diffraction (*24*)) in the Gd_2O_3 model compound. The labeled peaks represent Gd–O distances in the first coordination shell. The peak near 4 Å is due to many overlapping second-neighbor distances (Gd–Ca, Gd–Ti) at 3.2–4.5.

(EPR) data were obtained on powdered samples at room temperature and at 77°K. The spectra were obtained using an IBM ER200D spectrometer coupled to an ER041 MR microwave bridge and an ER4102ST cavity. Microwave frequencies were monitored using a Hewlett-Packard HP 5248-L counter and a HP 5257 transfer oscillator. The magnetic field was calibrated with a Bruker BNM-12 tracking magnetometer. Figure 3 shows the spectra for $(Ca_{0.995}Gd_{0.005})TiO_3$ and $(Ca_{0.925}Gd_{0.075})TiO_3$ at 77°K for magnetic fields between 0.03 and 0.67 T. The line positions in these spectra generally agree with those reported by Koopmans for gadolium-doped $CaTiO_3$, but our linewidths are somewhat broader (*17*).

TABLE IV

OBSERVED RAMAN FREQUENCIES FOR UNDOPED $CaTiO_3$

cm^{-1}	Relative peak intensity
155.8	0.20
182.2	0.52
225.6	0.36
246.8	1.00
285.9	0.24
337.3	0.15
471.3	0.25
494.6	0.08
640.1	0.09
676.1	0.09

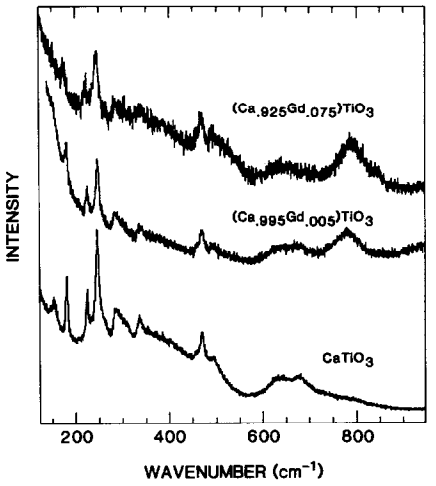

FIG. 2. Raman spectra of $(Ca_{1-x}Gd_x)TiO_3$, for $x = 0$, 0.005, and 0.075.

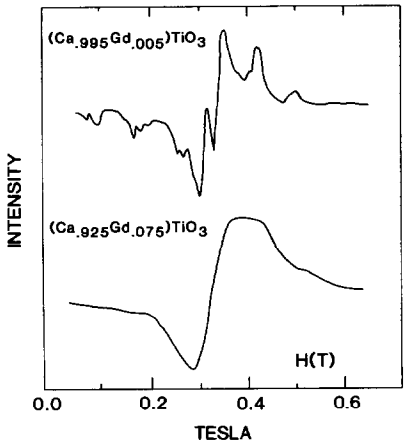

FIG. 3. Electron paramagnetic resonance spectra at 9.403 GHz and 77°K of $(Ca_{0.995}Gd_{0.005})TiO_3$ and $(Ca_{0.925}Gd_{0.075})TiO_3$.

X-ray fluorescence and scanning electron microscopy studies. X-ray fluorescence (XRF) data were obtained on powdered samples using a Rigaku Model 3064 wavelength dispersive instrument. Scanning electron micrographs (SEMs) were taken of powdered samples using an ISI Model DS-130 instrument. XRF analysis, EXAFS, electron paramagnetic resonance (EPR), and direct current emission spectra (Schwarzkopf Laboratories) showed the most abundant impurities to be Al, Fe, Mg, Si, and Sn at 0.01 to 0.10% levels. No impurity phases except a trace of rutile were detected by SEM. SEM also confirmed that approximately 7% Gd was present in the structure and uniformly distributed through the sintered matrix.

Discussion

Structural studies. The single-crystal X-ray refinement shows conclusively that, as expected, Gd^{3+} predominantly if not exclusively enters the Ca^{2+} site of $CaTiO_3$ under our preparative conditions. The final unit cell parameters (Table II) are within three standard deviations of those determined by powder neutron diffraction for pure $CaTiO_3$, consistent with the similarity of the ionic sizes of Ca^{2+} and Gd^{3+} (1.12 and 1.05 Å, respectively, in eight coordination) (*10, 11*). The detailed geometry within the structure of the doped perovskite is also essentially unchanged from that of pure $CaTiO_3$, the most important structural parameters differing by no more than about three standard deviations between the two structures. Using the precise structural data for undoped $CaTiO_3$ and Zachariasen's bond length–bond strength formulation, one can calculate a summed bond strength for Gd^{3+} of about 2.6 (ideally 3.0) for the 12 nearest-neighbor Gd–O bonds. This result indicates that the calcium site in $CaTiO_3$, as expected, is slightly too large to ideally accommodate Gd^{3+}.

The single-crystal X-ray study shows that the Ca(Gd) site is surrounded by eight near-neighbor oxygens (2.37–2.67 Å, mean 2.53 Å) and four next-neighbor oxygens (3.02–3.21 Å, mean 3.12 Å). For each Ca(Gd)–O distance the X-ray diffraction method, of course, gives the average over the structure.

The first-shell Gd–O distance as determined by EXAFS (Fig. 1) ranged from about 2.40 to 2.46 Å, depending upon how the transforms were weighted, the maximum value of k used, and the precise way in which the Gd–O phase was extracted and applied. The mean of these Gd–O distances is about 2.43 Å, shorter than the average diffraction derived distance by very nearly the difference in ionic radii of Ca^{2+} and Gd^{3+} in eight coordination (*10*). Since the EXAFS technique gives the Gd–O distance only at specific Gd-substituted sites averaged within each coordination shell, the difference between the X-ray diffraction Ca(Gd)–O and absorption Gd–O distances suggests that in $(Ca_{0.925}Gd_{0.075})TiO_3$ the coordination shell is slightly more contracted about the Gd^{3+} ions than about the Ca^{2+} ions. This result is understandable on the basis of the slightly smaller size and higher charge of Gd^{3+} compared to Ca^{2+}. Contraction about the dopant ions, in conjunction with charge-compensating cation vacancies, apparently produces local structural inhomogeneities which are especially prominent at high doping levels. At the 7.5% doping level, the gadolinium concentration is about 2 M and on average each gadolinium is within one unit cell of about two other gadoliniums. Unfortunately, since the EXAFS data was quite noisy at high wavevector (k) values, quantitative information regarding local disorder about Gd was not obtainable.

The Raman spectra support the hypothe-

sis of significant local structure modification at high doping levels (Fig. 2). The line shapes progressively broaden as the doping levels increase. Also, an additional broad band grows in near 780 cm^{-1} which most likely corresponds to a Ti–O stretching mode. Similar changes in Raman spectra as a result of dopant-induced defects have been noted earlier in related oxide structures (*18, 19*). Such effects also are seen in the EPR spectra (Fig. 3), presumably reflecting the consequences of site inhomogeneity as well as paramagnetic interactions between gadolinium sites.

Charge compensation mechanism. A variety of mechanisms were considered to account for the required charge compensation accompanying the substitution of Gd^{3+} into the Ca^{2+} sites.

1. Reduction of Gd^{3+} to Gd^{2+} could occur. However, Gd^{2+} has never been observed in any chemical system, in accord with the extremely unfavorable gadolinium III → II reduction potential (−3.9 V, estimated) (*20*). Furthermore, the nearly colorless nature of the highly doped samples, as well as the direct observation of Gd^{3+} by EPR, are consistent with the gadolinium being present predominantly, if not exclusively, as the trivalent ion.

2. Reduction of 7.5% of the Ti^{4+} ions to Ti^{3+} could occur. The lack of significant color in the highly doped samples and the failure to observe a Ti^{3+} EPR signal strongly argue against this possibility. However, the absence of a Ti^{3+} EPR signal cannot be taken as incontrovertible proof that this ion is not present in the doped samples. When Ti^{3+} is present in highly symmetric environment, it can have a rapid spin lattice relaxation time and not be observed under the experimental conditions described here or those described by Koopmans (*17, 21*). However, in the $CaTiO_3$ lattice, the titanium site has only approximate octahedral symmetry and the symmetry is expected to be reduced even further in the doped samples. The high-temperature, air-firing conditions of the synthesis also are not favorable for titanium reduction. For all the above reasons, charge compensation by Ti^{4+} reduction is considered an extremely unlikely possibility.

3. Charge compensation could be accomplished by substitution of low valent impurities. However, the purity of the starting materials and our analytical results on products suggest that the impurity levels are not nearly high enough for this mechanism to be important, at least for the highly doped products.

4. Excess oxygen could be present in interstitial sites. However, in $CaTiO_3$ the largest interstitial vacancies (centers of the [100] faces of the idealized cubic cell, diameter ca. 1.1 Å) are too small to accommodate an oxide ion (ionic radium 1.35 Å in two-coordination) (*10*). Therefore this model also seems unlikely.

5. Titanium vacancies (7.5%/4) could occur. A test refinement of the diffraction data in which the titanium occupancy parameter was varied did converge with a slightly reduced titanium occupancy of 97(1)%. However, the difference between the refined value and full occupancy is practically within experimental error. Neither this result nor our other measurements positively confirm the presence or absence of this mechanism. B-site-deficient perovskites are, however, well known (*22, 23*).

6. Calcium vacancies could occur. Again none of our measurements confirm or deny this possibility. A-site-deficient perovskites are well known, an outstanding example being ReO_3 in which the A-site is completely vacant (*22, 23*).

From the above considerations, we propose that the most likely charge compensation mechanism in $(Ca_{0.925}Gd_{0.075})TiO_3$ is by cation deficiency (Ca^{2+} and/or Ti^{4+}).

Conclusions

This study conclusively shows that Gd^{3+} enters the $CaTiO_3$ lattice under our preparative conditions by direct replacement of Ca^{2+}. The charge compensation mechanism is not established beyond doubt, but probably is accomplished by cation (Ca^{2+} and/or Ti^{4+}) vacancies. Evidence is presented that, although the average $CaTiO_3$ structure is virtually unaffected by high Gd^{3+} doping levels, there is considerable structural perturbation about sites substituted by gadolinium. This effect is ascribed to the slightly smaller size and higher charge of Gd^{3+} compared to Ca^{2+}, and possibly to charge compensation effects as well. Under comparable synthesis conditions other similarly sized trivalent (and possibly tetravalent) lanthanide and transuranic elements would be expected to enter the $CaTiO_3$ host in a similar way. Since trivalent *trans*-neptunium elements are slightly larger than Gd^{3+} (Ca^{2+} and Pu^{3+} have essentially identical sizes (*10*)), local site inhomogeneity might be somewhat less for these elements.

Acknowledgments

The work reported herein was partially done at SSRL which is supported by the Department of Energy, Office of Basic Energy Sciences, and the National Institutes of Health, Biotechnology Resource Program, Division of Research Resources. The portion of this work carried out by Los Alamos personnel was partially supported by the Department of Energy, Office of Basic Energy Sciences, Chemical Sciences Division. The work of F. W. Lytle and R. B. Greegor (Boeing Corporation) was supported by DOE Grant DE-FG0684ER45121. Michael Eastman was supported by a grant from the Robert A. Welch Foundation of Houston, Texas. The assistance of Dr. R. C. Hagan, Los Alamos group ESS-1, and Mr. J. D. Farr, Los Alamos group CLS-1, with the X-ray fluorescence and electron microscopy measurements is greatly appreciated. We gratefully acknowledge many enlightening discussions with Drs. R. A. Penneman, R. R. Ryan, B. I. Swanson, Steven Conradson, and W. H. Woodruff of Los Alamos National Laboratory.

References

1. A. E. RINGWOOD, V. M. OVERSBY, S. E. KESSON, W. SINCLAIR, N. G. WARE, W. O. HIBBERSON, AND A. MAJOR, *Nucl. Chem. Waste Manage.* **2,** 287 (1981); A. E. RINGWOOD, *Amer. Sci.* **70,** 201 (1982).
2. E. R. VANCE AND D. K. AGRAWAL, *Nucl. Chem. Waste Manage.* **3,** 229 (1982).
3. T. J. WHITE, R. L. SEGALL, AND P. S. TURNER, *Angew. Chem. Int. Ed. Eng.* **24,** 357 (1985).
4. F. MAZZI AND R. MUNNO, *Amer. Mineral.* **68,** 262 (1983).
5. N. ISHIZAWA, F. MARUMO, S. IWAI, M. KIMURA, AND T. KAWAMURA, *Acta Crystallogr. Sect. B* **38,** 368 (1982).
6. G. V. BAUZUEV AND G. P. SHVEIKIN, *Dokl. Akad. Nauk SSSR* **226,** 393 (1983).
7. M. NANOT, F. QUEYROUX, J. C. GILLES, AND R. PORTIER, *J. Solid State Chem.* **38,** 74 (1981).
8. C. R. A. CATLOW, A. V. CHADWICK, G. N. GREAVES, AND L. M. MORONEY, *Nature (London)* **312,** 601 (1984).
9. R. A. PENNEMAN AND P. G. ELLER, *Radiochim. Acta* **32,** 81 (1983).
10. R. D. SHANNON, *Acta Crystallogr. Sect. A* **32,** 751 (1976).
11. W. H. ZACHARIASEN, *J. Less-Common Met.* **62,** 1 (1978); W. H. ZACHARIASEN AND R. A. PENNEMAN, *J. Less-Common Met.* **69,** 369 (1980).
12. M. MAREZIO, J. P. REMEIKA, AND P. D. DERNIER, *Acta Crystallogr. Sect. B* **26,** 2008 (1970).
13. H. J. A. KOOPMANS, G. M. H. VAN DE VELDE, AND P. J. GELLINGS, *Acta Crystallogr. Sect. C* **39,** 1323 (1983).
14. "International Tables for X-Ray Crystallography," Vol. 4, Kynoch Press, Birmingham (1984).
15. A. C. LARSON, "Crystallographic Computing" (F. R. Ahmed, Ed.), pp. 291–294, Munksgaard, Copenhagen; A. C. LARSON, *Amer. Crystallogr. Assoc. Program Abstr. Ser. 2,* **5**(2), 67.
16. F. W. LYTLE, G. H. VIA, AND J. H. SINFELT, *in* "Synchrotron Radiation Research" (H. Winick and S. Doniach, Eds.), Chap. 12, pp. 401–424, Plenum, New York (1980).
17. H. J. A. KOOPMANS, "Simulation and Interpretation of ESR Powder Spectra of Some Gd^{3+} Doped Perovskites," Technishe Hogeschool Twente (1978).
18. D. MICHEL, M. PEREZ, Y. JORBA, AND R. COLLONGUES, *J. Raman Spectrosc.* **5,** 163 (1976).
19. V. G. KERAMIDAS AND W. B. WHITE, *J. Chem. Phys.* **59,** 1561 (1973); V. G. KERAMIDAS AND W. B. WHITE, *J. Phys. Chem. Solids* **34,** 1873 (1973).
20. L. J. NUGENT, R. D. BAYBARZ, J. L. BURNETT, AND J. L. RYAN, *J. Phys. Chem.* **77,** 1528 (1973).

21. D. KONIG, *in* "Physical Methods in Advanced Inorganic Chemistry" (H. A. O. Hill and P. Day, Eds.), Interscience, London (1968).

22. F. S. GALASSO, "Structure, Properties, and Preparation of Perovskite-type Compounds," Pergamon, New York (1969).

23. O. MULLER AND R. ROY, "The Major Ternary Structural Families," Springer-Verlag, New York (1974).

24. L. PAULING AND M. D. SHAPPELL, *Z. Kristallogr.* **75,** 128 (1930); D. H. TEMPLETON AND C. DAUBON, *J. Amer. Chem. Soc.* **76,** 5237 (1954).